Polymer Testing 129 (2023) 108268

Contents lists available at ScienceDirect

Polymer Testing

journal homepage: www.elsevier.com/locate/polytest

Side-chain Poly[2]pseudorotaxanes containing β-cyclodextrin for more sustainable tanning process

Ilaria Quaratesi [a,b,c], Immacolata Bruno [c], Antonio Pauciulo [c], Andrea R. Bartiromo [c], Elena Badea [b,d,**], Cristina Carşote [e], Placido Neri [a], Carmen Talotta [a], Rocco Gliubizzi [c,***], Valeria Di Tullio [f], Noemi Proietti [f], Antonuccio Cepparrone [g], Franca Nuti [g], Vittoria Ferrara [a,b,c], Carmine Gaeta [a,*]

[a] Dipartimento di Chimica e Biologia "A. Zambelli", Università di Salerno, Via Giovanni Paolo II 132, Fisciano, SA, I-84084, Italy
[b] National Research and Development Institute for Textile and Leather - Research Institute for Leather and Footwear (INCDTP-ICPI), Ion Minulescu Str. 93, Bucharest, 031215, Romania
[c] BI-QEM SPECIALTIES SPA, Zona Industriale, Buccino, SA, 84021, Italy
[d] Department of Chemistry, Faculty of Sciences, University of Craiova, Calea Bucuresti Str. 107 I, Craiova, 200512, Romania
[e] National Museum of Romanian History, Calea Victoriei Str. 12, Bucharest, 030026, Romania
[f] Istituto di Scienze del Patrimonio Culturale (ISPC) CNR, Area della Ricerca di Roma 1, Monterotondo (RO), 00015, Italy
[g] FGL International SPA, Via Provinciale Francesca Nord, 73, Castelfranco di Sotto (PI), 56022, Italy

ARTICLE INFO

Keywords:
Bio-based chemicals
β-cyclodextrin
Side-chain Poly[2]pseudorotaxanes
Tanning processes
Sustainability

ABSTRACT

Sustainability of leather lies in how the hide, a sustainable, naturally renewable, raw material, is processed. Tanning chemistry has been a limiting factor for leather sustainability. In this study, a host-guest synthesis strategy was selected to modify one of the most widely used tanning polymer, MIDA DD, and obtain a new hybrid tanning system containing β-cyclodextrin, and leather drastically less impactful on the earth and people. ***P***oly[2]pseudorotaxane ***S***ide-***C***hain ***C***omplexes (PSCCs) have been obtained by threading β-cyclodextrin units onto the side-chains of the commercial MIDA DD. The formation of PSCCs in aqueous solution was investigated by using 1D NMR, ATR-FTIR and TGA experiments. The ability of PSCCs to stabilize the collagen matrix was tested at laboratory and industrial pilot scale by micro-DSC, ATR-FTIR and solid-state NMR techniques. The physical and mechanical performance of the obtained crust leather was determined by standard tests used in tanning industry. Side-chain poly[2]pseudorotaxanes showed better tanning performances than the fossil-based MIDA DD, the most effective supramolecular tannins being obtained by mixing β-CD and MIDA DD in ratios close to 1/1 (w/w). The new tanning mixtures allow for significantly reducing both the amount of fossil-based MIDA-DD polymer in the current tanning processes (by 45%) and the free bisphenol content in leather crust (by more than 80%) due to the presence of bio-based β-CD in the composition of the new supramolecular tanning agents. The findings disclosed here pave the way for the CDs' employment in improving the sustainability of tanning processes.

1. Introduction

Europe counts for over 25% of the world leather production and stands out for possessing one of the largest and most active consumer marketplaces for leather goods. Chrome tanning, faster and cheaper than vegetable tanning, which takes more skill and labor, has dominated the leather-making industry for the past 100 years [1,2]. Chrome tanning, faster and cheaper than vegetable tanning, which takes more skill and labor, has dominated the leather-making industry for the past 100 years [1,2]. However, the potential oxidation of Cr(III) to Cr(VI), which is recognized as a human carcinogen [3–6], represent a significant risk for human health as well as water, land, air and their ecosystems [7–9].

* Corresponding author.
** Corresponding author. National Research and Development Institute for Textile and Leather - Research Institute for Leather and Footwear (INCDTP-ICPI), Ion Minulescu Str. 93, Bucharest, 031215, Romania.
*** Corresponding author.
E-mail addresses: elena.badea@edu.ucv.ro (E. Badea), rocco.gliubizzi@bi-qem.com (R. Gliubizzi), cgaeta@unisa.it (C. Gaeta).

https://doi.org/10.1016/j.polymertesting.2023.108268
Received 3 September 2023; Received in revised form 28 October 2023; Accepted 1 November 2023
Available online 7 November 2023

Consequently, chrome-free leather has become more and more appreciated by consumers and in increasing demand [10]. The use of organic-based tannins has therefore been considered a significant step toward more eco-friendly leather processing. On the other hand, the most commercially successful organic tannins are derived from non-renewable fossil sources [1,2,11,12]. Increasing the sustainability of tanning process depends on the partial or total substitution of fossil-based materials. Hybrid tannage does not require changing the current processing technology or replacing the equipment, being easily and quickly transferred to the industry.

Built on this premise, the selective complexation (molecular recognition [13]) of organic molecules, inside the hydrophobic cavity of water-soluble macrocycle such as cyclodextrins [14,15], could be a suitable method to synthetize a hybrid tannin and thus reduce the fossil-based tannin quantity in both leather and water and solid wastes. Molecular recognition in water [16] is the central topic of supramolecular chemistry, and the complexation of anionic and cationic guests [17], and organic pollutants has been intensively studied in environmental sciences. Cyclodextrins (CDs) [14,15] are water-soluble macrocyclic hosts which are able to host hydrophobic guests in their internal cavity and form inclusion complexes, improving water solubility of organic molecules and providing a wide range of industrial (i.e., food, pharmaceuticals, chemistry) and environmental applications [18–22]. CDs are cyclic oligosaccharides composed of six (α-CD), seven (β-CD) or eight (γ-CD) α-1,4-linked glucose units with a toroidal shape characterized by hydrophilic exterior rims and a hydrophobic cavity (Fig. 1). It was reported that CDs thread into the side-pendants of polymers bearing side-chains groups (Fig. 1) and form poly[2]pseudorotaxane architectures (side-chain poly[2]pseudorotaxanes, Fig. 1) [23,24]. Such supramolecular architectures have recently gained increasing interest due to inherent mechanical and physical properties, i.e. self-healing and stimuli-responsiveness [23–25].

In this paper, we studied the way in which MIDA DD, belonging to the dihydroxy diphenylsulphone compounds (Fig. 1) *and one of the most widely* used *tannin at present, could be complexed by* β-CD to obtain a hybrid tannin agent with significantly lower environmental impact.

MIDA DD consists of a water-soluble blend of fossil-based oligomers bearing sulfonated 4,4′-dihydroxydiphenyl sulphone moieties [26] as side chains (Fig. 1). It may therefore release bisphenol S (BPS) in leather. Bisphenol S is the most common bisphenol analog marketed as a bisphenol A-free product since BPA was restricted by several EU regulations and directives such as: REACH, Toy Safety Directive and Plastic Food Contact Materials Regulation. Bisphenols mainly enter the human body through contaminated food or water or by contact (i.e. with thermal paper in the form of sales receipts or with the leather goods). Recently, BPS was also shown to be toxic to the reproductive system and was to hormonally promote certain breast cancers at the same rate as BPA [27,28]. These are strong arguments to regulate BPS in exactly the same manner as BPA. It is expected that in the immediate future, the companies producing BPS-based organic tannins will have to comply with safety standards for BPS, too. The MIDA DD structure makes it a potential candidate for the synthesis of side-chain poly[2]pseudorotaxanes (Fig. 1) with β-CD as host. To achieve our purpose, we synthetized a side-chain poly[2]pseudorotaxane by threading β-CD macrocycles onto the sulfonated 4,4′-dihydroxydiphenyl sulphone pendants attached on the main chain of MIDA DD. The five different mixtures obtained by increasing the quantity of β-CD were fully characterized by ^{1}HNMR, ATR-FTIR and TG analysis. Their ability to interact with collagen and act as a tannin, i.e. to improve the hydrothermal stability of the chemical matrix collagen-tannin, was characterized by micro-DSC, NMR MOUSE and ATR-FTIR. The mechanical and physical properties of leather tanned with MIDA DD@β-CD side-chain poly[2]pseudorotaxane were tested using the standard test methods used in leather tanning industry and the results obtained proved its performing characteristics compared to standard leather obtained using MIDA DD. The new hybrid-tanning complex exploits the synergy between MIDA DD and β-CD allowing for substantially reducing both the amount of MIDA DD in the tanning process and of residual BPS in leather.

2. Experimental section

2.1. Materials

β-Cyclodextrin (β-CD) was purchased from Roquette (Kleptose® GC grade ≥93%) and used without further purification. 2DS basico, MIDA DD and sodium sulphate were provided by BI-QEM Specialties S.P.A. The mixture of dicarboxylic acids was purchased from BASF (commercial name: Sokalan® DCS. CAS number: 68603-87-2).

The sheep hides used for tanning tests on the laboratory scale were from Leather and Footwear Research Institute (ICPI) of the National Research and Development Institute for Textiles and Leather (INCDTP), Bucharest. Sodium chloride was purchased from Chimreactive S.R.L.

The calf hides, reagents (i.e., sodium chloride, IDROSIN JK®, HCOONa and ECOGRIN 30LR®) used in industrial pilot tanning process scale were provided by FGL International S.P.A., Italy.

2.2. Side-chain poly[2]pseudorotaxane mixtures preparation

Side-chain poly[2]pseudorotaxane mixtures, henceforth referred to as PSCCs, were obtained by mixing the MIDA DD precursor (2DS basico) and β-CD in weight ratios (Table 1) at 85 °C, under stirring, for 15 min. The mix of dicarboxylic acids (10%, w/w) and sodium sulphate (15%, w/w) was then added (in the same percentages used for the marketed MIDA DD tanning agent) and the mixture was further stirred until complete dissolution. The final product was dried in the oven at 80 °C. The pH of the 20% (w/w) solution of PSCC in distilled water was (4.5 ±

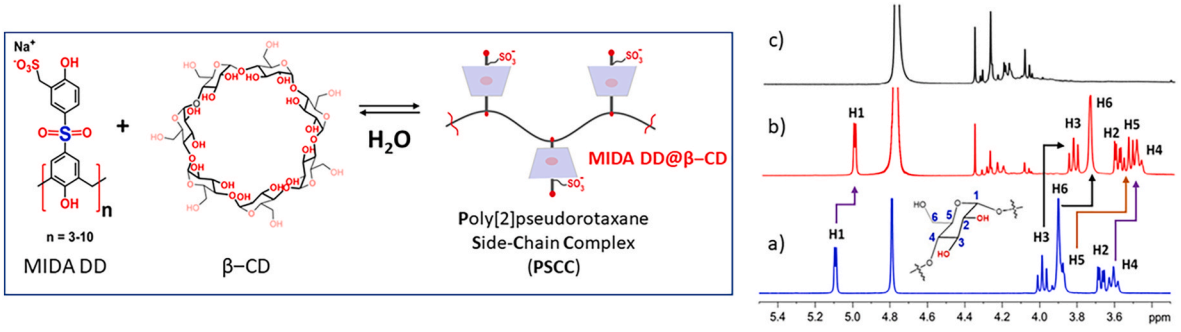

Fig. 1. (Left side) Cartoon representation of the side-chain poly[2]pseudorotaxane complex (PSCC) formation by complexation equilibrium between β−cyclodextrin (β−CD) molecules onto the side-chain units of MIDA DD polymer. (Right side) ^{1}H NMR spectra (400 MHz, 298 K, D_2O) of: a) β-CD (coloured in blue); b) free PSCC1 (coloured in red) and c) MIDA DD (coloured in black).". (For interpretation of the references to colour in this figure legend, the reader is referred to the Web version of this article.)

Table 1
Percentage weight composition (%) of the five PSCC mixtures.

	MIDA DD	PSCC1	PSCC2	PSCC3	PSCC4	PSCC5
β-Cyclodextrin	–	17.5	27	33.5	52.5	61.4
2DS basico	75	57.5	48	41.5	22.5	13.6
β-CD:2DS basico weight ratio (w/w)	–	0.3/1	0.6/1	0.8/1	2.3/1	4.5/1
Na_2SO_4	15	15	15	15	15	15
Dicarboxylic acids	10	10	10	10	10	10

0.5).

2.3. Characterization and test methods

Liquid state NMR was used to characterize the PSCC mixtures, while the collagen-PSCCs matrices were characterized by solid state NMR. 1D NMR spectra of PSCCs mixtures, MIDA DD and β-CD were recorded on 600 MHz [600 (1H) and 150 MHz (13C)], 400 MHz [400 (1H) and 100 MHz (13C)], and 300 MHz [300 (1H) and 75 MHz (13C)] spectrometers. The observed chemical shifts are reported relative to the residual solvent peak.

Thermogravimetric analysis (TGA) of PSCC mixtures, MIDA DD and β-CD was carried out with a TGA Q500 thermobalance (TA Instruments) with 1 μg resolution. Samples of about 7 mg were placed in open platinum pans and run under nitrogen purge (100 cm^3/min), in the temperature range (25–900) °C, at 10 °C min^{-1} heating rate.

Infrared Spectroscopy in Attenuated Total Reflection mode (FTIR-ATR) analysis was carried out for characterizing both the PSCC mixtures and PSCC-tanned leathers. Spectra were recorded with an ALPHA spectrophotometer (Bruker Optics) equipped with a Platinum ATR module, in the 4000–400 cm^{-1} spectral range, with a 4 cm^{-1} resolution, using 32 scans. Opus software (Bruker Optics, Germany) was used for the acquisition and elaboration of the spectra.

Micro-Differential Scanning Calorimetry (micro-DSC) was employed to characterize the stability of collagen-PSCCs matrices against thermal denaturation. Measurements were carried out with a high-sensitivity Micro-DSC III calorimeter (SETARAM) and were performed in the (25–90) °C temperature range, at 0.5 °C min^{-1} heating rate, using 850 μl stainless steel (Hastelloy C) cells. The very low scan rate provides the quasi-equilibrium condition for DSC analysis and allow an accurate measurement of the denaturation parameters. Samples of about 5.0 mg were suspended in 0.5 M acetate buffer (pH = 5.0) directly in the measure cell and left for 30 min to assure their fully hydration and avoid denaturation temperature and enthalpy variation with hydration level. Experimental DSC data acquired with the SETARAM SetSoft2000 software were analyzed using PeakFit 4.1 (Jandel Scientific). DSC multiple peaks were deconvoluted using the PeakFit asymmetric Gaussian fit function to improve the fit of the asymmetry in the peaks.

^{13}C CP-MAS NMR spectra of leather samples were obtained using a Bruker Avance III spectrometer operating at 100 MHz. The spin rate was 12 kHz. Leather samples were finely cut and packed into 4-mm zirconia rotors with an available volume reduced to 25 μl and sealed with Kel-F caps. Standard MIDA DD and β-CD were analyzed as received. ^{13}C CP-MAS spectra were acquired using a contact time for the cross polarisation of 1.5 ms, the recycle delay of 3 s and the 1H π/2 pulse width of 3.5 μs. The cross polarisation was achieved applying the variable spin-lock sequence RAMP–CP-MAS. The RAMP was applied on the 1H channel and, during the contact time, the amplitude of the RAMP was increased from 50% to 100% of the maximum value. Spectra were acquired with a time domain of 1024 data points with zero filled and Fourier transformed with a size of 4.096 data points applying an exponential multiplication with a line broadening of 32 Hz.

Both laboratory and industrial pilot scale tanning tests were performed using a wet-white technology, as reported in the SI.

The shrinkage temperature of leather samples was measured using a Giuliani Shrinkage *Tg* tester IG/TG, according to the standard method ISO 3380:2015 [IULTCS/IUP 16]. The physical-mechanical characteristics of leather samples as well as their colourfastness to light were determined according to the specific standard tests used in the tanning industry [UNI EN ISO 3380:2015, UNI EN ISO 2589: 2016, EN ISO 3376:2020, UNI EN ISO 3378: 2005, UNI EN ISO 3379: 2015, UNI EN ISO 105- B02:2014]. The content of free bisphenol S in crust leather was determined by liquid chromatography–mass spectrometry (LC–MS) after extraction with MeOH at 60 °C for 1 h [ISO/DIS 11936].

3. Results and discussion

3.1. Characterization of MIDA DD@β-CD side-chain poly[2] pseudorotaxanes

The formation of MIDA DD@*β*-CD side-chain poly[2]pseudorotaxane complex was demonstrated by a combination of investigations, including ^1H NMR spectroscopy, FTIR spectroscopy and TGA analysis. Previously, we showed that *β*-CD macrocycles can form *endo*-cavity complexes with 4,4′-dihydroxydiphenyl sulphone (4,4′-BPS) and 2,4′-dihydroxydiphenyl sulphone (2,4′-BPS) [29]. Investigations by isothermal titration *calorimetry* (ITC) and NMR indicated the formation of BPS@β-CD complexes with 1:1 stoichiometry by an enthalpically-driven inclusion process, which was accompanied by an unfavorable entropy change [29]. *Based on these insights,* the formation of MIDA DD@*β*-CD poly[2]pseudorotaxanes was studied by ^1H NMR spectroscopy (Fig. 1a–c), focusing on the complexation induced shifts (C.I.S., $\Delta\delta = \delta_{complex} - \delta_{free}$) experienced by the H-atoms of the *β*-CD (Fig. 1a–c). The ^1H NMR spectrum of the PSCC1, obtained by mixing *β*-CD:MIDA DD precursor in a 0.3:1 (*w/w*) ratio, illustrated in Fig. 1b, shown significant upfield shifts of the *β*-CD signals: H3 and H6 protons, shown a C.I.S. of −0.1 ppm, while H5-atom, shown a C.I.S. of −0.3. This result indicates the inclusion of sulfonated 4,4′-BPS side-chains inside the cavity of *β*-CD with a fast complexation equilibrium. Smaller C.I.S. were observed for H1, H2, and H4 protons of *β*-CD, namely −0.04, −0.027, and 0.02 ppm (Fig. 1). ^1H NMR spectra of PSCC2-PSCC5 mixtures are reported in SI (Fig. S1). Differently, the signals of MIDA DD were very little influenced by the formation of the pseudorotaxane motif.

The ATR-FTIR spectra of the five PSCCs mixtures were compared to those of the free host and guest and reported in Fig. 2 and Figure S2, SI. The spectra of PSCCs mixtures show the specific bands of MIDA DD, *β*−CD, sodium sulphate (619 and 1043 cm^{-1}) and dicarboxylic acids (1711 and 2946 cm^{-1}). The ATR-FTIR spectrum of *β*-CD shows the characteristic bands of the OH-groups at 3278 cm^{-1}, the C–H stretching vibrations at 2923 cm^{-1} and the C–O stretching vibrations at 1151, 1022, 997, 942 and 575 cm^{-1} [30]. The anomeric band at 858 cm^{-1} essentially consists of C_I–H deformation coupled to other motions [31]. All these bands are present in the spectra of PSCCs mixtures, some showing significant shifts i.e., the C–O stretching bands at 1151 and 1022 cm^{-1} are displaced at 1143 and 1027 cm^{-1}, respectively (Fig. 2 in red). The MIDA DD specific bands are visible at: 3233 cm^{-1} (OH stretching on the aromatic rings), 1585 cm^{-1} (C–C stretching of the aromatic rings), 1135 cm^{-1} (stretching signal of S–O), 695 cm^{-1} (S–C stretching) and 833 cm^{-1} (C–C bending of the aromatic ring) [32]. All these bands are present, slightly shifted, in the five PSCCs. This confirm that the interaction between MIDA DD and *β*−CD is H-bond based, as it doesn't affect the monomeric unit of the polymer.

The thermogravimetric analysis (TGA) was previously used by some of us [25,29] and other [33] to characterize inclusion complexes of *β*−CD. As expected, the thermograms of free *β*−CD indicate the occurrences of mass loss in three endothermic processes: mass loss due to the evaporation of water associated with the macrocycle at $T < 100$ °C (mass loss of about 10 %); significant mass loss related to *β*−CD degradation at $T \approx 321$ °C and a slow decomposition between 350 °C and 420 °C due to

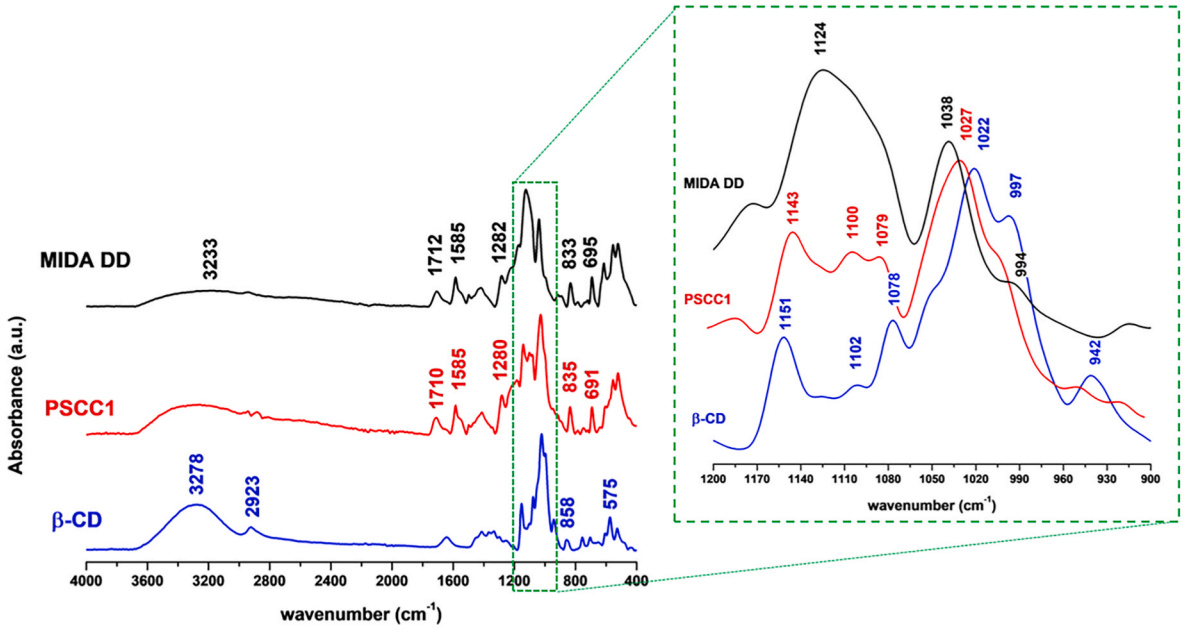

Fig. 2. (Left side) ATR-FTIR spectra of MIDA DD, PSCC1 and β-CD. (Right side) The zooming in of the (1200-900) cm^{-1} region highlights the MIDA DD and β-CD bands' shift as a result of their interaction to form PSCC1.

the thermal degradation of its "chair conformation" (Fig. 3) [34]. MIDA-DD also features three mass loss processes: the first, due to the presence of dicarboxylic acid, occurs at $T \approx 196$ °C, the second is a slow degradation occurring between 200 °C and 500 °C, followed by a fast decomposition at 630 °C (Fig. 3 and Fig. S3, SI).

As reported in Fig. 3, a reduction in mass loss due to superficial and internal water is observed as a result of host-guest complex formation in PSCC1. The enthalpy-rich water molecules filling the hydrophobic cavity of β−CD are released in the bulk upon guest inclusion. Interestingly, the water loss significantly decreases from PSCC1 to PSCC3 (characterized by β−CD/MIDA DD weight ratios of 0.3/1, 0.6/1 and 0.8/1), while for PSCC4 and PSCC5 (with β−CD/MIDA DD weight ratios of 2.3/1 and 4.5/1, respectively) this behaviour is much more toned down due to the excess of β−CD which no longer form inclusion complexes with MIDA DD (Fig. S3 and Fig. S4, SI). As expected, PSCC1-3 show thermal stability close to that of MIDA DD, while PSCC4-5 are less thermally stable. It is worth noting that PSCC1 is the only mixture showing higher thermal stability compared to MIDA DD: it degrades around 681 °C, while the degradation of the free polymer occurs at 638 °C.

3.2. *Tanning properties of β-CD@MIDA DD side-chain poly[2] pseudorotaxanes*

The strength and density of the interactions between the tannin molecules and collagen determine leather's hydrothermal stability [35–39], which is generally assessed by measuring the shrinkage temperature using the standard test UNI EN ISO 3380: 2015. However, temperature is an intensive parameter, which cannot explain the mechanism of the shrinkage temperature increasing. We used the micro-Differential Scanning Calorimetry (micro-DSC) technique to characterize the thermal denaturation [40,41] of the chemical collagen-tannin matrix and obtain a simultaneous qualitative and quantitative evaluation of the collagen-tannin interaction.

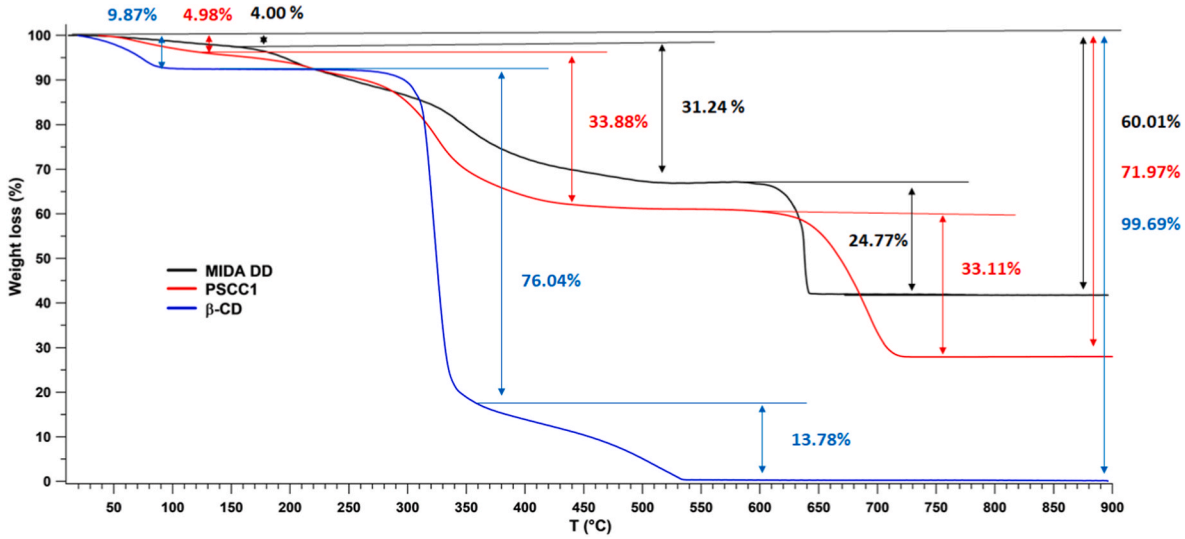

Fig. 3. TG thermograms of β-CD, PSCC1 and MIDA DD.

It is worth noting that a very good relationship between denaturation temperature and shrinkage temperature was previously reported by some of us [40]. The typical thermal denaturation peak of fibrous collagen within hide shown by micro-DSC is a narrow and symmetric endothermic peak, whose temperature of maximum heat flow, T_{max}, occurs in the range (50–60) °C (Fig. 4a), depending on animal species, age and on the anatomic part of the hide, i.e., shoulder, belly and butt [40,41]. For symmetrical peaks, corresponding to very homogeneous collagen materials (e.g., collagen solutions), T_{max} has been assumed as the denaturation temperature of collagen according to a statistical process [42]. However, collagen stabilization through tanning is most often a heterogeneous process since the tanning penetration into leather, a heterogenous porous material, is of a heterogeneous nature, too. Therefore, leather frequently exhibits broad and/or markedly asymmetric denaturation DSC peaks for which T_{max} does not reflect the denaturation temperature across the full scan. (Fig. 2b–h). Consequently, the temperature at the beginning of denaturation T_{onset} was considered more suitable to evaluate thermal stability of leather in such conditions [40]. The width at half height $\Delta T_{1/2}$ of the DSC endothermic peak provides a measure of the range of molecular thermal stabilities dispersion: its increase reflects the increase of thermal heterogeneity, suggesting the presence of various collagen populations with distinct thermal stability [41–46]. The experimental enthalpy of thermal denaturation, ΔH (J/g), measured as the area under the endothermic peak, represents the amount of energy needed to induce the denaturation of collagen matrix by disrupting the interactions that stabilize the triple helix, fibrillar and fibrous hierarchical structures. It therefore depends on both the hydration level and tannin type [41,47].

The deconvolution of broad asymmetric DSC peaks of leather tanned with the PSCC mixtures (Fig. 2d–h), allowed us to identify and quantify the various collagen populations with distinct thermal stabilities by assuming that the percent contribution to the overall denaturation enthalpy of each component of the endotherm is proportional to the percentage of the corresponding collagen population [40,48,49]. The denaturation parameters of collagen-PSCC1-5 matrices obtained by peak deconvolution are reported in Fig. 4 and Table 2 together with those for not-treated hide and MIDA DD- and β-CD-tanned hides.

The micro-DSC thermogram of the hide treated with β-CD shows a main denaturation peak at $T_1 = 54$ °C, as in the case of not tanned hide (Fig. 4a), with a shoulder at $T_2 = 61$ °C (Fig. 4b) representing the denaturation of the collagen fraction (about 32%) which interacted with β-CD. The remaining collagen (about 68%) is in a chemically unmodified state (not tanned). The denaturation peak of L-MIDA DD (Fig. 4c) shows the presence of two components corresponding to two thermally stabilized (chemically modified) collagen populations denaturing at $T_3 = 65$ °C (53%) and $T_4 = 73$ °C (47%), respectively. The micro-DSC denaturation peaks of the hides tanned with side-chain poly[2]pseudorotaxanes PSCCs (Fig. 4d–h) exhibit distinct denaturation patterns depending on the β-CD/MIDA DD ratio, as expected. Even though all are characterized by the presence of the thermally stabilized collagen

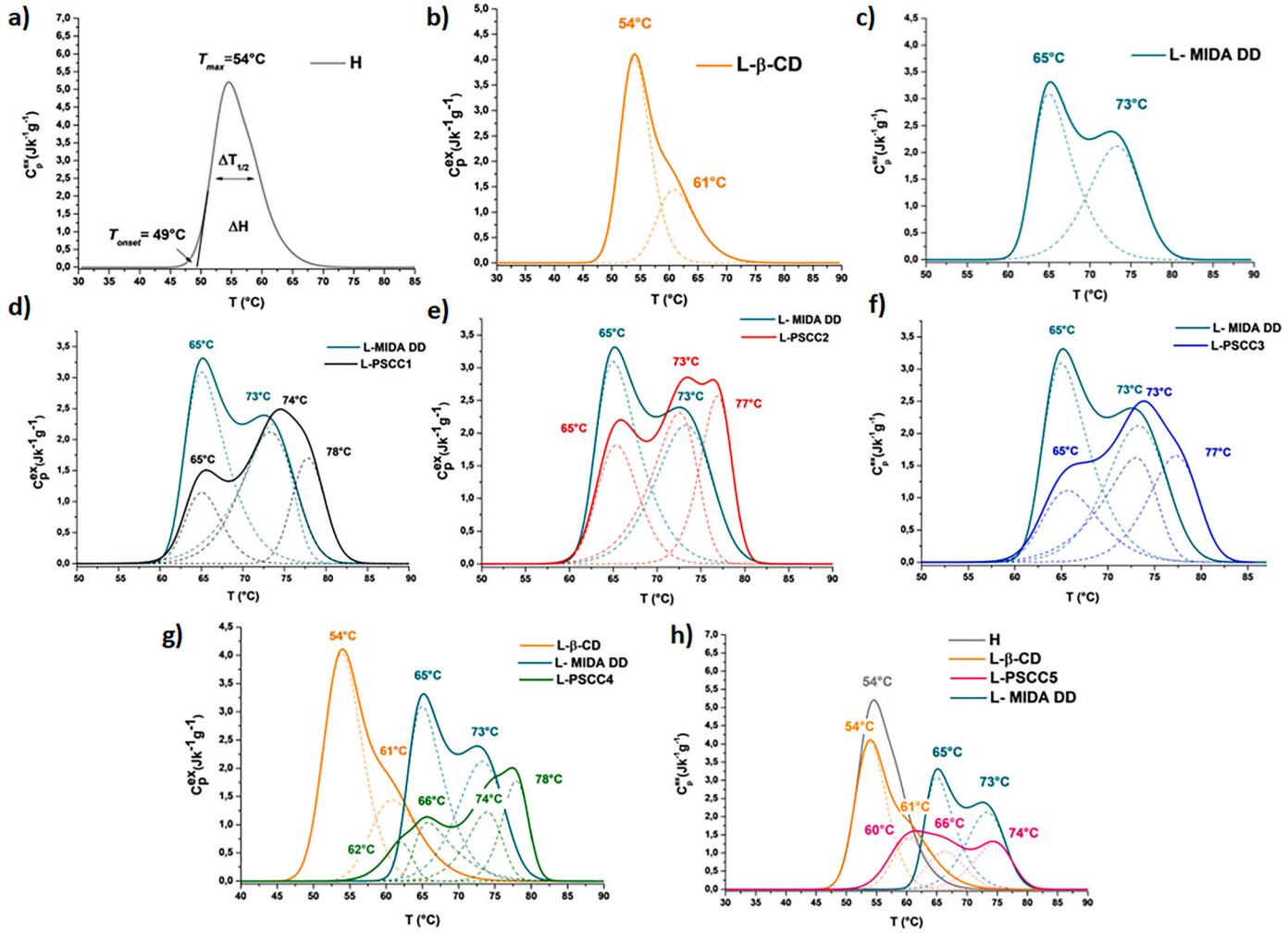

Fig. 4. Thermal denaturation peaks obtained by micro DSC in excess water at a heating rate of 0.5 K·min^{-1}for: (a) not tanned hide (H), (b to h) hide tanned with β-CD (L-β-CD), MIDA DD (L-MIDA DD); PSCC1 – PSCC5 mixtures (L-PSCC1 - L-PSCC5). For multi-component denaturation peaks, deconvolution into component peaks was applied.

Table 2
Micro-DSC parameters of thermal denaturation of collagen matrix within not-tanned hide and hides treated with β-CD, MIDA DD and PSCC1-5.

Sample/symbol[a]	T_{onset} (°C)	T_i^b (°C)	$\Delta T_{1/2}$ (°C)	$\Sigma\Delta H_i^c$ (J·g^{-1})	% ΔH_i^d
Not-tanned hide (H)	49	T_1 = 54	8.0	44.7	ΔH_1 = 100
L-β-CD	50	T_1 = 54 T_2 = 62	8.3	39.6	ΔH_1 = 68.3 ΔH_2 = 31.7
L-MIDA DD	62	T_3 = 65 T_4 = 73	12.8	37.1	ΔH_3 = 53.0 ΔH_4 = 47.0
L-PSCC1	62	T_3 = 65 T_4 = 74 T_5 = 78	15.5	36.2	ΔH_3 = 19.8 ΔH_4 = 53.9 ΔH_5 = 26.3
L-PSCC2	62	T_3 = 65 T_4 = 73 T_5 = 77	15.1	38.5	ΔH_3 = 28.0 ΔH_4 = 41.0 ΔH_5 = 31.0
L-PSCC3	62	T_3 = 65 T_4 = 74 T_5 = 78	14.7	36.4	ΔH_3 = 26.5 ΔH_4 = 38.0 ΔH_5 = 35.5
L-PSCC4	62	T_2 = 62 T_3 = 66 T_4 = 74 T_5 = 78	15.6	26.6	ΔH_2 = 12.9 ΔH_3 = 27.5 ΔH_4 = 28.6 ΔH_5 = 31.0
L-PSCC5	54	T_1 = 60 T_3 = 66 T_4 = 74	20.5	29.9	ΔH_1 = 37.9 ΔH_3 = 27.6 ΔH_4 = 34.5

populations present in L-MIDA DD, a collagen population showing higher denaturation at about 77–78 °C was identified in L-PSCC1-4, while a less stable collagen populations with denaturation temperature lower than 62 is present in L-PSCC4-5. The most thermally stable population denaturing at 77–78 °C could easily be assigned to the interaction of collagen with the macrocycle side-chain poly[2]pseudorotaxane MIDA DD@β-CD. The percentage of its enthalpy increases as the β-CD/MIDA DD ratio increases and approaches 1/1, then decrease for L-PSCC-4 and becomes zero for L-PSCC5. These findings suggest that a β-CD/MIDA DD ratio closer to 1/1, as for PSCC2 and PSCC3, significantly improves the hydrothermal stability of the chemical collagen-matrix. On the other hand, when the β-CD/MIDA DD ratio is higher than 1/1, the ability of PSCC4 and PSCC5 to stabilize the collagen matrix decreased due to the excess of β-CD, as clearly indicated by the peak component corresponding to collagen-β-CD population occurring at 62 °C in L-PSCC4 and at 60 °C in L-PSCC5 (Fig. 4g–h and Table 2). In addition, the most stable collagen population denaturing at about 78 °C is no longer present in the L-PSCC5 denaturation pattern. The micro-DSC results demonstrate that PSCC1-4 side-chain poly[2]pseudorotaxane mixtures have a superior thermal stabilization effect compared to MIDA DD since about (26–36) % of collagen reaches a more stable conformation upon denaturation. From the analysis of thermal denaturation patterns it follows that the optimal yield for the synthesis of PSCC host-guest complex is reached for the β-CD:MIDA DD weight ratio of 1/0.8, which corresponds to the PSCC3 mixture.

Interestingly, the denaturation temperature of leathers tanned with MIDA DD and PSCC1-3 ranges from 75 to 85 °C, similar to that of vegetable-tanned leather, while the denaturation enthalpy is higher compared to that of vegetable-tanned leathers (which ranges from 20 to 30 J g^{-1}), but still much lower compared with chrome-tanned leather (which reaches 50 J g^{-1}) [40,41,45,46]. It is therefore very likely that MIDA DD@β-CD poly[2]pseudorotaxanes interact with collagen through multiple hydrogen bonding due to its hydrogen bond donor groups, i.e., phenol and alcohol groups of MIDA DD and β-CD, respectively. Because of their flexibility, the phenolic hydroxyl of PSCCs' side chains are more likely to interact with the side chains of collagen polypeptide chains.During these linking phase, poly[2]pseudorotaxanes displace the interfibrillar water molecules [37,39] while the bulky cyclodextrins threaded along the sidechain of MIDA DD are wrapped into the interfibrillar space. Since water fills the inter-fibrillar spaces and bulges them, expanding the lattice, the accommodation of the PSCC guest-host complex seems to reduce the ability of collagen to be inflated by the action of water. According to Covington "link-lock tanning mechanism" [37], both MIDA DD and MIDA DD@β-CD poly[2]pseudorotaxanes tanning gives the hides moderate thermal stability due to the labile interactions that occur through the formation of hydrogen bonds between the phenolic/hydroxil groups of tannins and the polypeptide chains of the protein. This "link tanning mechanism" illustrated in Fig. 5 is in agreement with the polymer in a box model which demonstrated that cross-linking collagen causes an increase in its denaturation temperature due to a decrease in the degree of hydration which, in turn, determines the reduction of the size of the lattice, that is, the size of the box of the polymer model in a box [49].

Solid-state NMR and ATR-FTIR spectroscopy were also performed to characterize the interaction between the side-chain poly[2]pseudorotaxanes (PSCC) and collagen, and support the conclusions of the micro-DSC analysis.

3.3. ATR-FTIR characterisation of leather samples L-PSCCs

The FTIR-ATR spectra of the leather samples (L-PSCC1-5) tanned with the five PSCC1-5 mixtures are reported in SI, Fig. S5. All spectra present both the main bands of collagen and PSCCs (previously discussed and illustrated in Fig. 2). The FTIR-ATR spectrum of L-PSCC1 together with the spectra of raw hide and PSCC1 are presented in Fig. 6a–c, where the PSCC fingerprint region (1000–1800) cm^{-1} is highlighted and further processed using the second derivative method (Fig. 6d–f). The enhanced resolution of absorption peaks in the second derivative spectra allowed us to better separate the overlapping peaks (Fig. 6d–f).

The spectrum of leather tanned with PSCC1 (L-PSCC1) shows the typical signals of PSCC1 i.e., 1588 cm^{-1} (C–C stretching of the phenolic rings), 1142 cm^{-1} (S–O stretching) and 835 cm^{-1} (C–C–C bending) and the sharp peak at 1027 cm^{-1} (C–O stretching). The same bands were observed in L-PSCC2-5 leathers (Fig. S5, SI), confirming the penetration of PSCCs in the leather structure. It's worth noting that L-PSCC5 (Fig. S5, SI) spectrum shown very attenuated bands at 833 and 1586 cm^{-1}. This very well correlates with the micro-DSC results that indicated L-PSCC5 as having the lowest linking ability for collagen.

3.4. NMR solid state characterisation of leather samples L-PSCCs

The solid-state 13C CP-MAS NMR technique is a powerful tool for characterizing solid materials, and collagenous material.[51–53] It was shown that the 13C CP-MAS spectrum of leather provide a 'fingerprint' of the solid component of collagen, while allowing for tannin-type identification and the assessment of tanning process.53 Due to the aromatic/polysaccharide nature of tanning agents, there is essentially no overlap between the resonance bands of tannins and collagen signals when compared to ATR-FTIR. In Fig. 7, we report the 13C CP-MAS

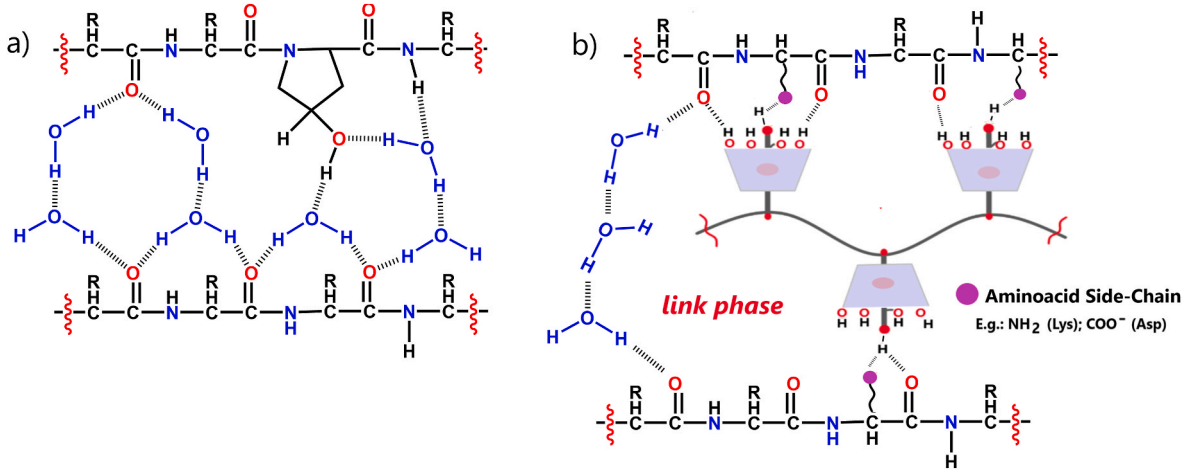

Fig. 5. a) Proposed model of hydrogen bonds and water bridges [37] involving the hydroxyl group of hydroxyproline Hyp and carbonyl groups in collagen polypeptide chains [49,50]. (b) Cartoon representation of a "linking" [36] pattern involving hydrogen bond donor groups of β-CD@MIDA DD side-chain poly[2]pseudorotaxanes and side chains of collagen.

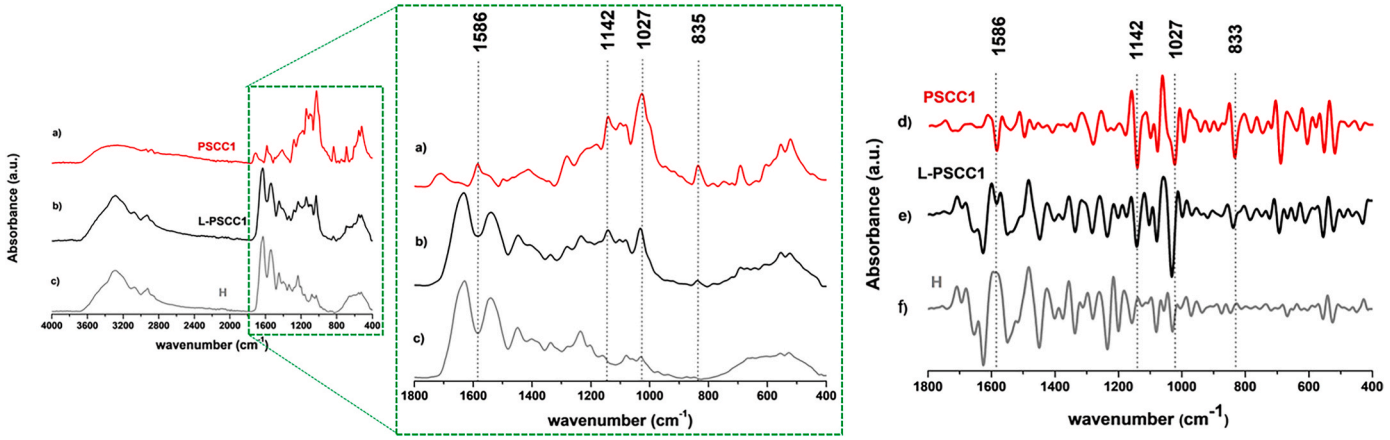

Fig. 6. (Left side) ATR-FTIR spectra of (a) PSCC1, (b) L-PSCC1, and (c) raw hide (H) and the zoom in of the PSCC fingerprint region (1000–1800) cm-1. (Right side) ATR-FTIR second derivative spectra in the PSCC fingerprint region (1000–1800) cm-1 for: (d) PSCC1, (e) L-PSCC1, (f) raw hide (H).

spectra of the sheep hides tanned with β−CD (Fig. 7b), MIDA DD (Fig. 7e) and PSCC3 (Fig. 7c) compared with those of raw hide (Fig. 7d) and the two precursors of PSCC3, i.e., standard β-CD (Fig. 7a), and MIDA DD (Fig. 7f). The spectrum of raw hide was assigned based on previously reported data.53 Resonances in the range 0–70 ppm (peaks from 6 to 20) are attributable to some functional groups of major amino acid residues. In detail, the peak at 71 ppm was assigned to the C-4 carbon atom of hydroxyproline (peak 6), the overlapped signals at 60 ppm were attributed to the C-2 carbon atoms of both hydroxyproline and proline, and the sharp peak at 43 ppm was attributed to the C2 of glycine. Other signals observed in Fig. 7d, are most probably attributable to the two common polyforms of CaCO3, namely, aragonite, at 171 ppm, and calcite, at 168.7 ppm.53 CaCO3 is used in hide liming, one of the main steps carried out during leather production in the tannery. In Fig. 7b and e, the spectra of the hides tanned with β-CD (L-β-CD) and MIDA DD (L-MIDA DD) are reported. They show the absorption bands corresponding to both the raw hide and tanning agent, easy to identify since they appear in distinct regions compared to raw hide fingerprint region, i.e. β-CD, in the range 70–110 ppm (Fig. 7b), and MIDA DD, in the range 110–160 ppm (Fig. 7e). The spectra of leathers tanned with PSCC3 (Fig. 7c), PSCC1 (Fig. S6a, SI), PSCC5 (Fig. S6c, SI) show the characteristics NMR signals of both the raw hide and the two precursor of PSCCs, i.e., β−CD and MIDA DD, thus confirming thus confirming the presence of PSCCs molecules inside the hide structure and their interaction with collagen.

3.5. *Industrial pilot scale tests: characterisation of L-PSCCi samples by standard methods*

The tanning effectiveness of the PSCCs mixtures was tested at industrial pilot scale on hide batches of 4 kg, as described in the SI. The shrinkage temperature Ts of the leather obtained with PSCC1-5 was measured (Table S1, SI) using the conventional standard test UNI EN ISO 3380: 2015. The data reported in Table S1 indicate higher shrinkage temperatures for L-PSCC1, L-PSCC2, and L-PSCC3 compared to the leather tanned with MIDA DD. Differently, L-PSCC4 showed a slightly reduced shrinkage temperatures of 68 °C, while for PSCC5 (4.5/1 w/w β-CD/MIDA DD ratio) the Ts value got very close to that of raw hide (56 °C), indicating almost no interaction with collagen. These results agree with the micro-DSC results reported in Table 2.

Based on the physical-chemical results previously described, only L-PSCC1, L-PSCC2, and L-PSCC3 leather samples were selected for the standard physical-mechanical tests and colourfastness. It is well known that the physical and mechanical properties of crust (not-finished) leather determine the potential applications of leather. The results reported in Table 3 show the suitability of L-PSCC1, L-PSCC2, and L-PSCC3 leathers to substitute the leather currently produced using MIDA DD for footwear production. Tensile strength determines the structural

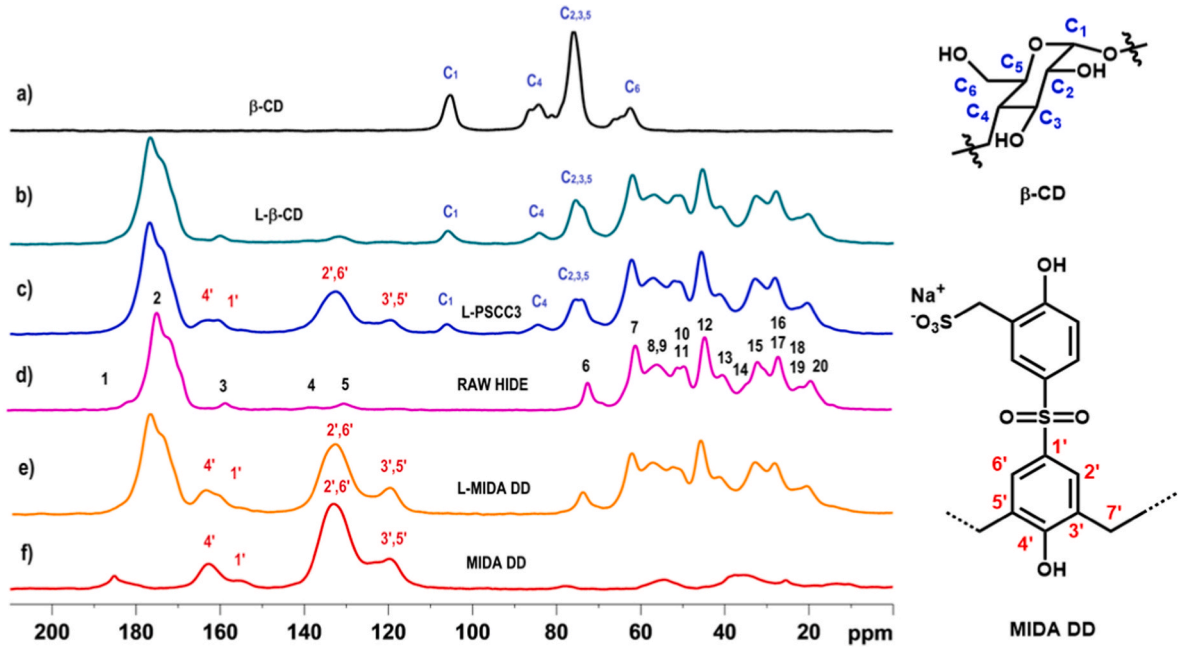

Fig. 7. Solid-state ^{13}C CP-MAS NMR spectra with the assignment of all resonances for: (a) β-CD; (b) hide tanned with β-CD; (c) hide tanned with PSCC3; (d) raw hide, (e) hide tanned with MIDA DD; (f) MIDA DD.

Table 3
Leather physical and mechanical standard tests.

Crust leather sample	L-MIDA DD	L-PSCC1	L-PSCC2	L-PSCC3	Standard method
T_s^a (°C)	70	74	72	75	UNI EN ISO 3380: 2015
Thickness[b] (mm)	1.6	1.7	1.5	1.8	UNI EN ISO 2589: 2016
Tensile strength (N/mm^2)[c]	23.2	25.1	33.9	32.9	EN ISO 3376:2020
Percentage elongation (%)[d]	34.6	37.0	39.3	41.0	EN ISO 3376:2020
Resistance to grain cracking (Kg)[e]	35.6	34.1	43.2	49.2	UNI EN ISO 3378: 2005
Crack index[f] (mm)	5.9	6.7	8.0	8.6	UNI EN ISO 3378: 2005
Force at crack[g] (Kg)	73.3	80.3	85.1	88.4	UNI EN ISO 3379: 2015
Distention and strength of the grain[h] (mm)	10.2	10.1	9.6	9.8	UNI EN ISO 3379: 2015
Colour fastness[i] (grey scale)	2/3 (24h) 2/3 (48h) 2 (72h)	2/3 (24h) 2/3 (48h) 2 (72h)	2/3 (24h) 2/3 (48h) 2 (72h)	2/3 (24h) 2/3 (48h) 2 (72h)	UNI EN ISO 105- A03:2019

(a)T_s = Shrinkage temperature: https://www.iso.org/standard/61792.html. (b) ISO 2589:2016 specifies a method for determining the thickness of leather. The method is applicable to all types of leather of any tannage. https://www.iso.org/standard/68859.html. (c and d) Tensile strengthat a specified load and elongation at maximum force of leather. https://www.iso.org/standard/75173.html. (e and f) ISO 3378:2002 specify a method for determining the resistance of leather to grain cracking and for determining the grain crack index. (g and h) ISO 3379:2015 specify a test method for the determination of distension and strength of the leather grain or finished surface. This method is applicable to all flexible leathers, and it is particularly suitable to determine the stability of leathers for footwear uppers. (i) ISO 105-A03:2019 specifies a method for determining the effect on colour due to the action of an artificial light source similar to natural daylight (D65):https://www.iso.org/standard/65209.html

resistance of leather to tensile forces hence its state and usability. Elongation determines leather flexibility and elasticity and highlights its deformation capacity during using. The more flexible the leather, the more the appearance of cracks and tears is avoided during the use. Moreover, high elasticity allows leather to withstand the elongation stresses during use. The distension at grain crack test is intended particularly for use with shoe upper leather where it gives an evaluation of the grain resistance to cracking during top lasting of the shoe uppers.

The color fastness to artificial light, which closely approximates to natural daylight, indicate a similar behavior of the analyzed leathers, regardless the tanning agent.

Overall, the newly synthesized PSCC1-3 supramolecular tannins provided leather with superior mechanical characteristics compared to the commercial leather tanned with MIDA DD, while reducing the fossil source (namely 2DS basico) up to 45%. Much more important, the free bisphenol S content of crust leather significantly decreased as reported in Table 4.

Considering the w/w β-CD/2DS basico ratio and the measured free bisphenol S content, it comes out that the reduction of the amount of free bisphenol is much higher than expected. In fact, if one considers the amount of fossil source in PSCC1 (57.5%) and in MIDA DD (75%), the expected final value of free-BPS in L-PSCC1 should be 6801 ppm, whereas the measured value is almost 4000 ppm lower (Table 4). It is worth noting that the effective decrease of BPS, i.e. the real final content, for PSCC3 in leather is 83% less compared to the leather obtained with MIDA DD. This is because the side-chain poly[2]pseudorotaxanes PSCCs penetrate and bind to the collagen matrix more efficiently than the commercial tannin MIDA DD. Our findings indicate that MIDA DD trapped in the cavity of β-CD becomes more stable, it binds to collagen more effectively and does not degrade to BPS (during either the tanning

Table 4
Free bisphenol S content of leather.

Sample	β-CD %	2DS basico%	Free BPS (ppm)
L-MIDA DD	0	75	8871
L-PSCC1	17.5	57.5	2820
L-PSCC2	27	48	2077
L-PSCC3	33.5	41.5	1489

process or extraction as per ISO regulation) as commercial MIDA DD does. This is supported by the shift in the constituent collagen population ratio toward the more stable ones (i.e., those corresponding to the collagen-PCCS chemical matrices) for the leathers tanned with PCCS1-3 against MIDA DD.

4. Conclusions

Side-chain poly[2]pseudorotaxanes PSCCs were obtained by molecular recognition of sulfonated 4,4-BPS side-chain of MIDA DD, inside the cavity of bio-based β-CD macrocycles. Five side-chain poly[2]pseudorotaxanes PSCC1-5 were obtained by mixing β-CD and the precursor of MIDA DD in different weight ratios (0.3/1, 0.6/1, 0.8/1, 2.3/1, and 4.5/1). The formation of the supramolecular systems was confirmed by 1D NMR, TGA, and FTIR-ATR analyses. The ability of PSCCs to interact with collagen and generate a stable collagen-tannin matrix was tested by micro-DSC analysis, ATR-FTIR and solid state NMR spectroscopy. Noteworthy, the β-CD/MIDA DD ratio significantly influenced the PSCCs ability to stabilize the collagen matrix. Industrial pilot scale tests were performed for the most effective supramolecular tannins PSCC1-3 (β-CD/MIDA DD weight ratios of 0.3/1, 0.6/1, and 0.8/1). The new leather obtained showed better thermal stability than the commercial leather L-MIDA DD, both in terms of denaturation/shrinkage temperature, as well as in the percentage of collagen population with the highest thermal stability. The physical-mechanical characteristics of the new leather, as well as its colour fastness, evaluated by the standard methods used in tanning industry, were better than those of commercial leather tanned with MIDA DD.

The presence of bio-based β-CD component in the PSCCs supramolecular systems allows for significantly reducing both the amount of fossil-based MIDA DD polymer in the tanning process and bisphenol S free content in leather crust. The PSCC3 shows the highest decrease of free BPS on leather, up to 83%.

Considering the current enormous interest in the synthesis and study of novel bio-based materials for greener tanning processes, and the excellent tanning ability of the side-chain type pseudorotaxane complexes here described, it can be expected that the presented results pave the way to a quick uptake of these materials in the tanning industry.

Associated content

The Supporting Information is available free of charge at:

Detailed experimental section: ^{1}H NMR and ATR-FTIR spectra of PSCCs; TG-DTG thermograms of PSCCs; ATR-FTIR spectra of not tanned and tanned hides; Procedure for laboratory and pilot scale tanning tests; Shrinkage temperature determined by standard test.

Author contributions

The manuscript was written through contributions of all authors. All authors have given approval to the final version of the manuscript.

Declaration of competing interest

The authors declare that they have no known competing financial interests or personal relationships that could have appeared to influence the work reported in this paper.

Data availability

Data will be made available on request.

Acknowledgements

Ilaria Quaratesi thanks the Regione Campania for the PhD Grant within “Dottorati di Ricerca con Caratterizzazione Industriale” DGR n. 156 del March 21, 2017 P.O.R. CAMPANIA FSE 2014/2020 – ASSE III – Obiettivo Specifico 14 Azione 10.4.5: POR D44J18000310006, and the Leather and Footwear Research Institute (INCDTP-ICPI) of Bucharest for giving her access to the laboratory and microproduction infrastructures of the Research Leather Department. The authors also acknowledge the University of Salerno for facilitating the use of the 600 MHz NMR spectrometer. It is also acknowledged the support of the Agritech National Research Center and funding from the European Union NextGenerationEU through PIANO NAZIONALE DI RIPRESA E RESILIENZA (PNRR) – MISSIONE 4 COMPONENTE 2, INVESTIMENTO 1.4 – D.D. 1032 17/06/2022, CN00000022. Elena Badea acknowledges the grant of the Ministry of Research, Innovation and Digitalization, CNCS/CCCDI-UEFISCDI, project number PN-III-P3-3.5-EUK-2019-0236, within PNCDI III. This manuscript reflects only the authors’ views and opinions, neither the European Union nor the European Commission can be considered responsible for them.

Appendix A. Supplementary data

Supplementary data to this article can be found online at https://doi.org/10.1016/j.polymertesting.2023.108268.

Abbreviations

PSCC	***P***oly[2]pseudorotaxane ***S***ide-***C***hain ***C***omplex
β-CD	β-cyclodextrin
BPA	Bisphenol A
BPS	Bisphenol S

References

[1] A.D. Covington, Modern tanning chemistry, Chem. Soc. Rev. 26 (2) (1997) 111, https://doi.org/10.1039/cs9972600111.
[2] A.D. Covington, W.R. Wise, Tanning Chemistry the Science of Leather, The Royal Society of Chemistry: homas Graham House, Science Park, Milton Road, Cambridge, CB4 0WF, UK, 2019.
[3] H. Sun, J. Brocato, M. Costa, Oral chromium exposure and toxicity, Curr. Environ. Health Rep. 2 (3) (2015) 295–303, https://doi.org/10.1007/s40572-015-0054-z.
[4] M. Velusamy, B. Chakali, S. Ganesan, F. Tinwala, S. Shanmugham Venkatachalam, Investigation on pyrolysis and incineration of chrome-tanned solid waste from tanneries for effective treatment and disposal: an experimental study, Environ. Sci. Pollut. Res. 27 (24) (2020) 29778–29790, https://doi.org/10.1007/s11356-019-07025-6.
[5] J. Liang, X. Huang, J. Yan, Y. Li, Z. Zhao, Y. Liu, J. Ye, Y. Wei, A review of the formation of Cr(VI) via Cr(III) oxidation in soils and groundwater, Sci. Total Environ. 774 (2021), 145762, https://doi.org/10.1016/j.scitotenv.2021.145762.
[6] A. Sh. Sallam, A.R.A. Usman, H.A. Al-Makrami, M.I. Al-Wabel, A. Al-Omran, Environmental assessment of tannery wastes in relation to dumpsite soil: a case study from riyadh, Saudi arabia, Arabian J. Geosci. 8 (12) (2015) 11019–11029, https://doi.org/10.1007/s12517-015-1956-7.
[7] S.J. Ali, J.R. Rao, B.U. Nair, Novel approaches to the recovery of chromium from the chrome-containing wastewaters of the leather industry, Green Chem. 2 (6) (2000) 298–302.
[8] A. Moretto, Hexavalent and trivalent chromium in leather: what should Be done? Regul. Toxicol. Pharmacol. 73 (2) (2015) 681–686, https://doi.org/10.1016/j.yrtph.2015.09.007.
[9] K. Chojnacka, D. Skrzypczak, K. Mikula, A. Witek-Krowiak, G. Izydorczyk, K. Kuligowski, P. Bandrów, M. Kułażyński, Progress in sustainable technologies of leather wastes valorization as solutions for the circular economy, J. Clean. Prod. 313 (2021), 127902, https://doi.org/10.1016/j.jclepro.2021.127902.
[10] Y.S. Hedberg, Chromium and leather: a review on the chemistry of relevance for allergic contact dermatitis to chromium, J. Leather Sci. Eng. 2 (1) (2020) 20, https://doi.org/10.1186/s42825-020-00027-y.
[11] J. Ammenn, C. Huebsch, E. Schilling, B. Dannheim, Chemistry of syntans and their influence on leather quality, J. Am. Leather Chem. Assoc. 110 (11) (2015) 349–354.
[12] Y. Yu, Y. Lin, Y. Zeng, Y. Wang, W. Zhang, J. Zhou, B. Shi, Life cycle assessment for chrome tanning, chrome-free metal tanning, and metal-free tanning systems, ACS Sustain. Chem. Eng. 9 (19) (2021) 6720–6731, https://doi.org/10.1021/acssuschemeng.1c00753.
[13] C. Gaeta, C. Talotta, F. Farina, G. Campi, M. Camalli, P. Neri, Conformational features and recognition properties of a conformationally blocked calix[7]Arene derivative, Chem. Eur J. 18 (4) (2012) 1219–1230, https://doi.org/10.1002/chem.201102179.
[14] J. Szejtli, Introduction and general overview of cyclodextrin chemistry, Chem. Rev. 98 (5) (1998) 1743–1754, https://doi.org/10.1021/cr970022c.

[15] G. Crini, Review: a history of cyclodextrins, Chem. Rev. 114 (21) (2014) 10940–10975, https://doi.org/10.1021/cr500081p.
[16] R. Del Regno, G.D.G. Santonoceta, P. Della Sala, M. De Rosa, A. Soriente, C. Talotta, A. Spinella, P. Neri, C. Sgarlata, C. Gaeta, Molecular recognition in an aqueous medium using water-soluble prismarene hosts, Org. Lett. 24 (14) (2022) 2711–2715, https://doi.org/10.1021/acs.orglett.2c00819.
[17] C. Gaeta, T. Caruso, M. Mincolelli, F. Troisi, E. Vasca, P. Neri, P-Sulfonatocalix[7] Arene: synthesis, protolysis, and binding ability, Tetrahedron 64 (22) (2008) 5370–5378, https://doi.org/10.1016/j.tet.2008.03.017.
[18] N. Sharma, A. Baldi, Exploring versatile applications of cyclodextrins: an overview, Drug Deliv. 23 (3) (2016) 729–747, https://doi.org/10.3109/10717544.2014.938839.
[19] A. Alsbaiee, B.J. Smith, L. Xiao, Y. Ling, D.E. Helbling, W.R. Dichtel, Rapid removal of organic micropollutants from water by a porous β-cyclodextrin polymer, Nature 529 (7585) (2016) 190–194, https://doi.org/10.1038/nature16185.
[20] W. Chen, X. Liu, X. Zhang, Slow-Release Type Leather Fragrance Finishing Agent and Preparation Method Thereof, 2013. CN101857908B, March 20.
[21] K. Yang, L. Chen, L. Zhuo, G. Huang, Z. Li, Fragrant Artificial Leather and Preparation Method Thereof, 2015. CN103114459B, March 18.
[22] K. Köse, M. Tüysüz, D. Aksüt, L. Uzun, Modification of cyclodextrin and use in environmental applications, Environ. Sci. Pollut. Res. 29 (1) (2022) 182–209, https://doi.org/10.1007/s11356-021-15005-y.
[23] A. Harada, Y. Takashima, M. Nakahata, Supramolecular polymeric materials via cyclodextrin–guest interactions, Acc. Chem. Res. 47 (7) (2014) 2128–2140, https://doi.org/10.1021/ar500109h.
[24] Y. Tan, SooWhan Choi, J.W. Lee, Y.H. Ko, K. Kim, Synthesis and characterization of novel side-chain pseudopolyrotaxanes containing cucurbituril, Macromolecules 35 (18) (2002) 7161–7165, https://doi.org/10.1021/ma020534f.
[25] C. Capacchione, P. Della Sala, I. Quaratesi, I. Bruno, A. Pauciulo, A.R. Bartiromo, P. Iannece, P. Neri, C. Talotta, R. Gliubizzi, C. Gaeta, Poly(Ethylene glycol)/β-cyclodextrin pseudorotaxane complexes as sustainable dispersing and retarding materials in a cement-based mortar, ACS Omega 6 (18) (2021) 12250–12260, https://doi.org/10.1021/acsomega.1c01133.
[26] P. Monti, Q. Migheli, A.R. Bartiromo, A. Pauciulo, R. Gliubizzi, S. Marceddu, P. A. Serra, G. Delogu, A storage-dependent platinum functionalization with a commercial pre-polymer useful for hydrogen peroxide and ascorbic acid detection, Sensors 19 (11) (2019) 2435, https://doi.org/10.3390/s19112435.
[27] M. Thoene, E. Dzika, S. Gonkowski, J. Wojtkiewicz, Bisphenol S in food causes hormonal and obesogenic effects comparable to or worse than bisphenol A: a literature review, Nutrients 12 (2) (2020) 532, https://doi.org/10.3390/nu12020532.
[28] M.S.H. Akash, S. Rasheed, K. Rehman, M. Imran, M.A. Assiri, Toxicological evaluation of bisphenol analogues: preventive measures and therapeutic interventions, RSC Adv. 13 (31) (2023) 21613–21628, https://doi.org/10.1039/D3RA04285E.
[29] I. Quaratesi, P. Della Sala, C. Capacchione, C. Talotta, S. Geremia, N. Hickey, R. Gliubizzi, I. Bruno, C. Sgarlata, R. Migliore, C. Gaeta, P. Neri, Selective recognition of bisphenol S isomers in water by β-cyclodextrin, Supramol. Chem. 33 (6) (2021) 295–308, https://doi.org/10.1080/10610278.2021.1991925.
[30] C. Bruijnes, R. Bosman, P. Bareman, A. Besemer, in: D.G. Cameron (Ed.), Conformational Analysis of Starch Derivatives by FTIR Spectroscopy, Fairfax, VA, 1989, p. 342, https://doi.org/10.1117/12.969491.
[31] O. Egyed, Spectroscopic studies on β-cyclodextrin, Vib. Spectrosc. 1 (2) (1990) 225–227, https://doi.org/10.1016/0924-2031(90)80041-2.
[32] R. Ullah, X. Wang, Molecular vibrations of bisphenol "S" revealed by FTIR spectroscopy and their correlation with bisphenol "A" disclosed by principal component analysis, Appl. Opt. 57 (18) (2018) D20, https://doi.org/10.1364/AO.57.000D20.
[33] F. Giordano, C. Novak, J.R. Moyano, Thermal analysis of cyclodextrins and their inclusion compounds, Thermochim. Acta 380 (2) (2001) 123–151.
[34] F. Trotta, M. Zanetti, G. Camino, Thermal degradation of cyclodextrins, Polym. Degrad. Stabil. 69 (3) (2000) 373–379, https://doi.org/10.1016/S0141-3910(00)00084-7.
[35] F. Cappa, I. Paganoni, C. Carsote, M. Schreiner, E. Badea, Studies on the effect of dry-heat ageing on parchment deterioration by vibrational spectroscopy and micro hot table method, Polym. Degrad. Stabil. 182 (2020), 109375, https://doi.org/10.1016/j.polymdegradstab.2020.109375.
[36] A.D. Covington, L. Song, O. Suparno, H.E.C. Koon, M.J. Collins, Link-lock: an explanation of the chemical stabilisation of collagen, J. Soc. Leather Technol. Chem. 92 (1) (2008) 17.
[37] W.A.M. Madhavi, S. Weerasinghe, G.D. Fullerton, K.I. Momot, Structure and dynamics of collagen hydration water from molecular dynamics simulations: implications of temperature and pressure, J. Phys. Chem. B 123 (23) (2019) 4901–4914, https://doi.org/10.1021/acs.jpcb.9b03078.
[38] A.D. Covington, The mechanism of chrome tanning, Glob. J. Inorg. Chem. 1 (2) (2010) 119–131.
[39] J. Bella, B. Brodsky, H.M. Berman, Hydration structure of a collagen peptide, Structure 3 (9) (1995) 893–906, https://doi.org/10.1016/S0969-2126(01)00224-6.
[40] C. Carsote, E. Badea, Micro differential scanning calorimetry and micro hot table method for quantifying deterioration of historical leather, Herit. Sci. 7 (1) (2019) 48, https://doi.org/10.1186/s40494-019-0292-8.
[41] C. Carşote, E. Badea, L. Miu, G.D. Gatta, Study of the effect of tannins and animal species on the thermal stability of vegetable leather by differential scanning calorimetry, J. Therm. Anal. Calorim. 124 (3) (2016) 1255–1266, https://doi.org/10.1007/s10973-016-5344-7.
[42] C.E. Weir, Rate of shrinkage of tendon collagen: heat, entropy, and free energy of activation of the shrinkage of untreated tendon; effect of acid, salt, pickle, and tannage on the activation of tendon collagen, J. Res. Natl. Bur. Stand. 42 (1) (1949) 17, https://doi.org/10.6028/jres.042.002.
[43] E. Onem, A. Yorgancioglu, H.A. Karavana, O. Yilmaz, Comparison of different tanning agents on the stabilization of collagen via differential scanning calorimetry, J. Therm. Anal. Calorim. 129 (1) (2017) 615–622, https://doi.org/10.1007/s10973-017-6175-x.
[44] H.R. Tang, A.D. Covington, R.A. Hancock, Use of DSC to detect the heterogeneity of hydrothermal stability in the polyphenol-treated collagen matrix, J. Agric. Food Chem. 51 (23) (2003) 6652–6656, https://doi.org/10.1021/jf034380u.
[45] C. Carsote, C. Şendrea, M.-C. Micu, A. Adams, E. Badea, Micro-DSC, FTIR-ATR and NMR MOUSE study of the dose-dependent effects of gamma irradiation on vegetable-tanned leather: the influence of leather thermal stability, Radiat. Phys. Chem. 189 (2021), 109712, https://doi.org/10.1016/j.radphyschem.2021.109712.
[46] A. Cucos, C. Gaidau, E. Badea, L. Miu, Influence of glycerin on denaturation temperature of chrome- and vegetable-tanned leather, Rev. Roum. Chem. 60 (2015) 1093.
[47] M. Luescher, M. Rüegg, P. Schindler, Effect of hydration upon the thermal stability of tropocollagen and its dependence on the presence of neutral salts: tropocollagen thermal stability, Biopolymers 13 (12) (1974) 2489–2503, https://doi.org/10.1002/bip.1974.360131208.
[48] E. Badea, G. Della Gatta, T. Usacheva, Effects of temperature and relative humidity on fibrillar collagen in parchment: a micro differential scanning calorimetry (micro DSC) study, Polym. Degrad. Stabil. 97 (3) (2012) 346–353, https://doi.org/10.1016/j.polymdegradstab.2011.12.013.
[49] C.A. Miles, M. Ghelashvili, Polymer-in-a-Box mechanism for the thermal stabilization of collagen molecules in fibers, Biophys. J. 76 (6) (1999) 3243–3252.
[50] G.I. Makhatadze, P.L. Privalov, Energetics of protein structure, in: Advances in Protein Chemistry, vol. 47, Elsevier, 1995, pp. 307–425, https://doi.org/10.1016/S0065-3233(08)60548-3.
[51] A.E. Aliev, Solid-state NMR studies of collagen-based parchments and gelatin, Biopolymers 77 (4) (2005) 230–245, https://doi.org/10.1002/bip.20217.
[52] F.H. Romer, A.P. Underwood, N.D. Senekal, S.L. Bonnet, M. Duer, D.G. Reid, J. H. Van Der Westhuizen, Tannin fingerprinting in vegetable tanned leather by solid state NMR spectroscopy and comparison with leathers tanned by other processes, Molecules 16 (2) (2011) 1240–1252, https://doi.org/10.3390/molecules16021240.
[53] N. Proietti, V. Di Tullio, C. Carsote, E. Badea, ^{13}C solid-state NMR complemented by ATR-FTIR and micro-DSC to study modern collagen-based material and historical leather, Magn. Reson. Chem. (2020), https://doi.org/10.1002/mrc.5024.